BOTANY

Glutamate triggers long-distance, calcium-based plant defense signaling

Masatsugu Toyota[1,2,3]*, Dirk Spencer[2]†, Satoe Sawai-Toyota[2]‡, Wang Jiaqi[1], Tong Zhang[4,5]§, Abraham J. Koo[4,5], Gregg A. Howe[6,7], Simon Gilroy[2]*

Animals require rapid, long-range molecular signaling networks to integrate sensing and response throughout their bodies. The amino acid glutamate acts as an excitatory neurotransmitter in the vertebrate central nervous system, facilitating long-range information exchange via activation of glutamate receptor channels. Similarly, plants sense local signals, such as herbivore attack, and transmit this information throughout the plant body to rapidly activate defense responses in undamaged parts. Here we show that glutamate is a wound signal in plants. Ion channels of the *GLUTAMATE RECEPTOR–LIKE* family act as sensors that convert this signal into an increase in intracellular calcium ion concentration that propagates to distant organs, where defense responses are then induced.

P lants respond within minutes to stresses such as wounding with both local and system-wide reactions that prime non-damaged regions to mount defenses. For herbivory, production of the defense hormone jasmonic acid (JA) and accumulation of toxic, repellent, or digestibility-reducing compounds all aid in deterring future attacks (1). Reactive oxygen species, electrical signals, and changes in cytosolic $Ca^{2+}$ concentration ($[Ca^{2+}]_{cyt}$) are thought to form signaling networks supporting both local and systemic defense responses [reviewed in (2)]. The electrical component is dependent on glutamate receptor–like (GLR) proteins (3–5), a family of cation-permeable ion channels that function in plant processes ranging from pathogen defense to root growth [reviewed in (6)]. Here we asked how GLRs are triggered by wounding and how subsequent Ca^{2+}-related signaling events operate to mediate systemic defense.

Caterpillar feeding on an *Arabidopsis* plant expressing the GCaMP3 fluorescent protein–based $[Ca^{2+}]_{cyt}$ sensor (7) revealed an increase in $[Ca^{2+}]_{cyt}$ at the herbivory site within 2 s that was transmitted over 1 to 2 min to distal leaves (Fig. 1A and movie S1). The spread was most evident in the vasculature, especially once the caterpillar severed a major vein. This $[Ca^{2+}]_{cyt}$ signal moved from older to younger leaves and vice versa (fig. S1 and movie S2). Wounding with scissors also caused a rapid $[Ca^{2+}]_{cyt}$ increase that propagated to distal leaves (Fig. 1B, fig. S2, and movie S3), indicating that herbivore chemical signals are not required. Mechanical wounding in leaf n [leaves numbered from oldest to youngest; fig. S3 (3)] led to $[Ca^{2+}]_{cyt}$ changes preferentially propagating to leaves $n \pm 3$ and $n \pm 5$ (table S1), paralleling previously defined patterns of wound-activated surface potential changes [WASPs (3)].

We wounded leaf 1 and monitored systemic responses in the "target" leaf 6 and "nontarget" leaf 5 to characterize this system. Upon wounding leaf 1, a $[Ca^{2+}]_{cyt}$ increase propagated at 1089 ± 141 µm/s to leaf 6 (Fig. 1C and fig. S4), where a subsequent Ca^{2+} increase spread across the organ (movies S3 and S4), expression of defense marker genes increased (Fig. 1D and fig. S5), and JA and JA-Ile accumulated (Fig. 1E). The $[Ca^{2+}]_{cyt}$ increase velocity mirrors that of both WASPs (3) and a postulated systemic jasmonate production trigger (8, 9). Phloem can transport long-distance signals

Fig. 1. Wounding triggers long-distance transmission of $[Ca^{2+}]_{cyt}$ increases and systemic defense responses. (**A**) Caterpillar (dashed outline) feeding (white arrow) caused local $[Ca^{2+}]_{cyt}$ increases (red arrowhead) that propagated toward younger leaves (yellow arrowheads). (**B**) Cutting leaf 1 (L1, white arrow, 0 s) caused a local $[Ca^{2+}]_{cyt}$ increase (red arrowhead) that propagated toward target distal leaves (yellow arrowheads), e.g., leaf 6 (L6), but not to nontarget leaves such as L5. (**C** to **E**) $[Ca^{2+}]_{cyt}$ signature (C), defense gene induction (D), and JA and JA-Ile accumulation (E). $N = 10$ (C), $N = 6$ (D), and $N = 3$ (E) separate experiments. Error bars, mean ± SE. *$P < 0.05$ leaf 6 versus 5. Scale bars, 1 mm (A) or 5 mm (B).
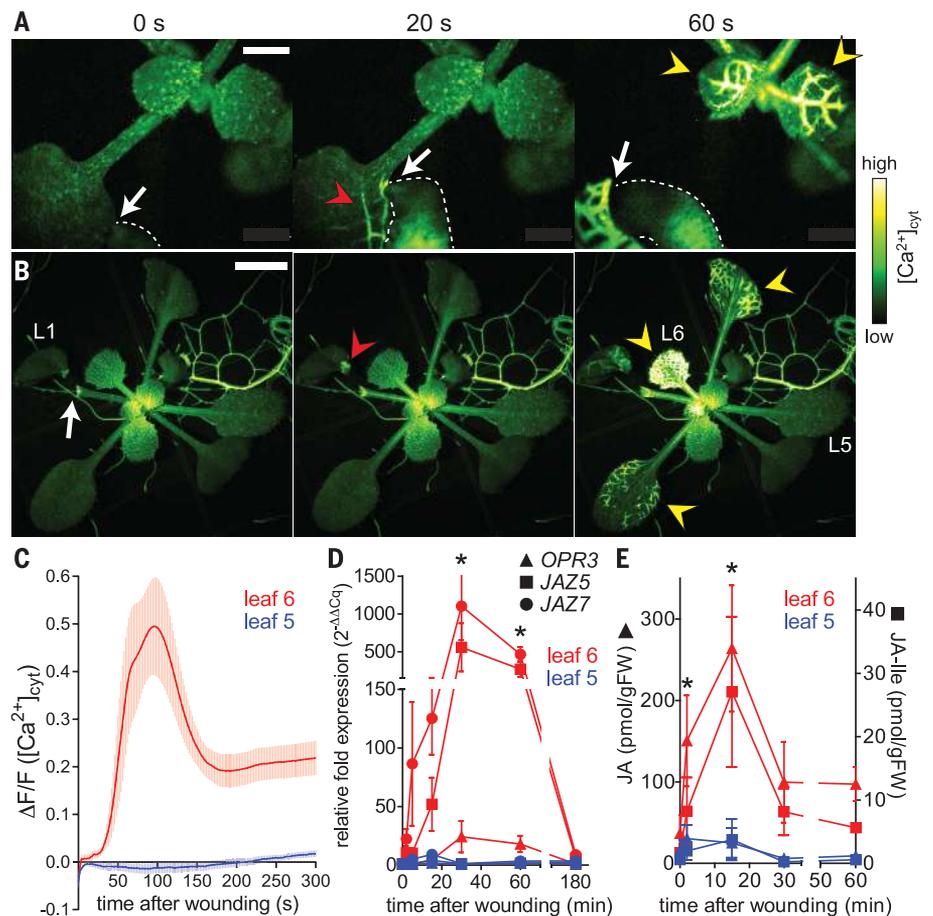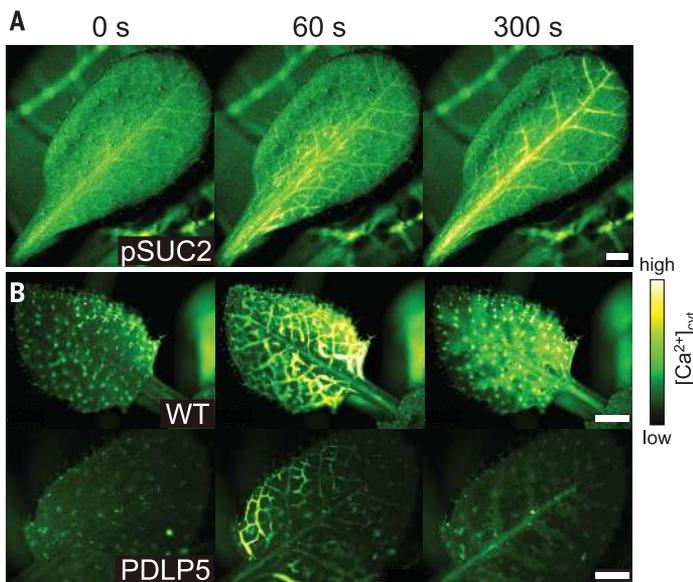
Fig. 2. Transmission of [Ca²⁺]$_{cyt}$ increases through the phloem and plasmodesmata. (**A**)Phloem-specific Ca²⁺ imaging in target leaf 6 upon mechanical wounding of leaf 1 (0 s). (**B**) [Ca²⁺]$_{cyt}$ increases in leaf 6 of wild-type (WT) and PDLP5 overexpression (OE) lines after cutting leaf 1 (0 s). (**C**) [Ca²⁺]$_{cyt}$ change in leaf 6 of wild-type and PDLP5 OE and (**D**) defense gene induction in leaf 5 and 6 after cutting leaf 1 in PDLP5 OE. The wild-type data from leaf 6 in Fig. 1, C and D, are reproduced (gray lines) to aid in comparison. Error bars, mean ± SE. $N > 7$ separate experiments. *$P < 0.05$. Scale bars, 1 mm.

(10, 11); visualizing [Ca²⁺]$_{cyt}$ in phloem and companion cells using the SUC2 promoter to selectively express GCaMP3 in these tissues revealed [Ca²⁺]$_{cyt}$ phloem signal propagation at 996 ± 207 μm/s (Fig. 2A, fig. S6, and movie S5). Pretreating the petiole of the wounded leaf with the Ca²⁺ channel inhibitor La³⁺ prevented both export of the [Ca²⁺]$_{cyt}$ increase (fig. S7) and systemic induction of wound-related marker genes (fig. S7D), suggesting that propagation of the [Ca²⁺]$_{cyt}$ change is required for induction of systemic responses.

The propagating [Ca²⁺]$_{cyt}$ increase slowed when spreading across the target leaf (fig. S8 and movies S3 and S4). We hypothesized that this phase of transmission might be propagated through plasmodesmata [(PD)] (12). Overexpression of PLASMODESMATA-LOCATED PROTEIN 5 (PDLP5) and knockout of PD-associated β-1,3-glucanase both impair PD conductance (13, 14); whereas neither of these disrupted the rapid leaf-to-leaf transmission of the [Ca²⁺]$_{cyt}$ increase, both limited the subsequent spread in target leaves to regions adjacent to the vasculature (Fig. 2, B and C, fig. S9, and movie S6). Wound-induced systemic gene expression was also
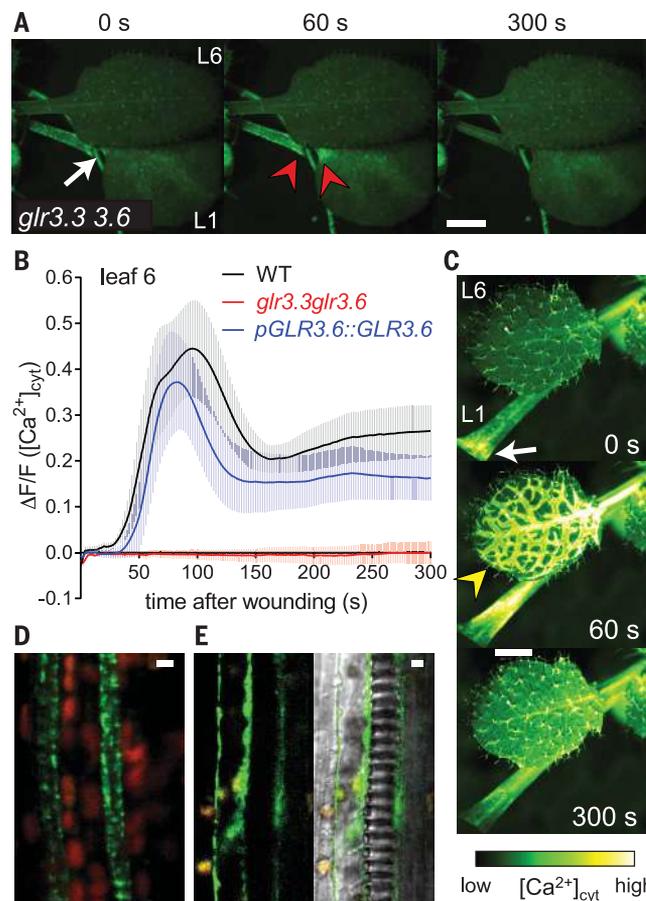
¹Department of Biochemistry and Molecular Biology, Saitama University, Saitama 338-8570, Japan. ²Department of Botany, University of Wisconsin, Madison, WI, 53593, USA. ³JST, PRESTO, Saitama 332-0012, Japan. ⁴Department of Biochemistry, University of Missouri, Columbia, MO 65211, USA. ⁵Interdisciplinary Plant Group, University of Missouri, Columbia, MO 65211, USA. ⁶Department of Energy–PRL, Michigan State University, East Lansing, MI 48824, USA. ⁷Department of Biochemistry and Molecular Biology, and Plant Resilience Institute, Michigan State University, East Lansing, MI 48824, USA.
*Corresponding author. Email: mtoyota@mail.saitama-u.ac.jp (M.T.); sgilroy@wisc.edu (S.G.) †Present address: Department of Biology, Stanford University, Stanford, CA 94305, USA. ‡Present address: Leica Microsystems, Tokyo 169-0075, Japan. §Present address: College of Agriculture, South China Agricultural University, Guangdong, China.
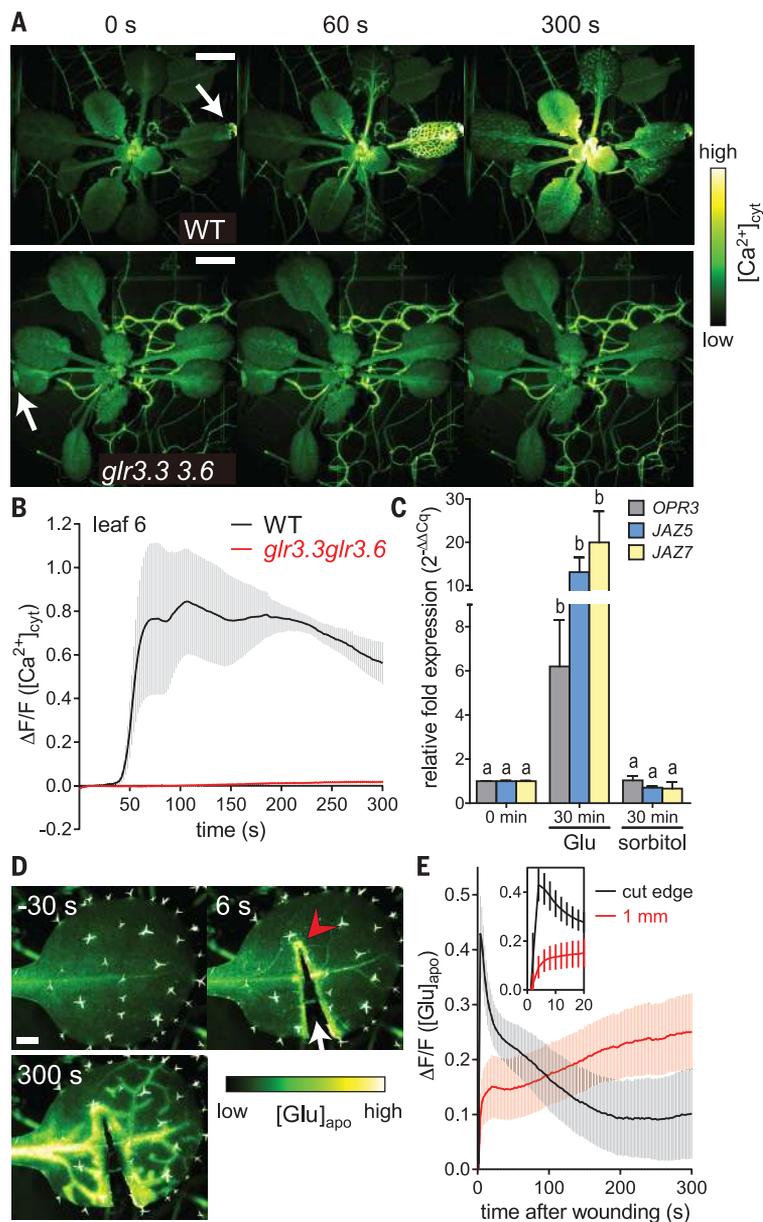

Fig. 3. GLR3.3 and GLR3.6 support long-distance transmission of [Ca²⁺]$_{cyt}$ increases.
(**A**) Cutting leaf 1 (L1; white arrow, 0 s) caused local [Ca²⁺]$_{cyt}$ increases (red arrowheads) that were not propagated toward distal leaves in glr3.3 glr3.6. (**B**) [Ca²⁺]$_{cyt}$ in the target leaf 6 (L6) of wild-type, glr3.3 glr3.6 mutants, and its rescued line. Error bars, mean ± SE. $N > 7$ separate experiments. Wild-type data from Fig. 1C are reproduced to aid in comparison. (**C**) Wound-induced [Ca²⁺]$_{cyt}$ in L6 of glr3.3 glr3.6 pGLR3.6::GLR3.6-EGFP lines. (**D**) Localization of GLR3.3 and (**E**) GLR3.6 in longitudinal sections of leaf petioles (see also fig. S11 for transverse section). Green, GFP; red, autofluorescence; blue, callose (aniline blue staining) showing sieve plate. Scale bars, 2 mm (A), 5 μm [(D) and (E)].

Fig. 4. Apoplastic Glu triggers systemic $[Ca^{2+}]_{cyt}$ changes and defense responses. (**A**) Application of 100 mM Glu (white arrow, 0 s) caused transmission of $[Ca^{2+}]_{cyt}$ increases to almost all leaves in wild type but not in the *glr3.3 glr3.6* mutants. (**B** and **C**) $[Ca^{2+}]_{cyt}$ (B) and defense gene induction (C) in leaf 6 after 100 mM Glu or sorbitol application to leaf 1. (**D**) $[Glu]_{apo}$ levels using iGluSnFR. Cutting leaf 1 (arrow, 0 s) caused an immediate increase in $[Glu]_{apo}$ at the wound, which gradually spread throughout the leaf. (**E**) iGluSnFR signals at the cut surface and 1 mm from the wound site (initial changes shown magnified in inset). Error bars, mean ± SE. $N > 5$ (B), $N > 4$ (C), and $N = 11$ (E) separate experiments. Letters a, b denote statistical differences ($P < 0.05$). Scale bars, 5 mm (A) or 1 mm (D).

in wounding responses (*16*). By contrast, expressing *pGLR3.6::GLR3.6-EGFP* in the *glr3.6* mutant (where it also rescues the knockout phenotype; Fig. 3, B and C) showed localization to the contact cells of the xylem parenchyma (Fig. 3E and fig. S11). These same cells show expression of the lipoxygenase isoform (*LOX6*) responsible for wound-related systemic jasmonate production (*17*). The observation that the two GLRs supporting long-distance $[Ca^{2+}]_{cyt}$ signaling are expressed in distinct locations suggests either that there may be chemical or electrical coupling between these cell types, or that two parallel but independent pathways exist for the wound signal in phloem and xylem parenchyma.

The GLRs are gated by amino acids [reviewed in (*6*)]; application of 100 mM L-Glu, but not other amino acids or sorbitol (osmotic control), resulted in plant-wide *GLR3.3/GLR3.6*–dependent systemic $[Ca^{2+}]_{cyt}$ increases (Fig. 4, A and B, fig. S12, and movies S9 and S10) and defense gene induction (Fig. 4C and fig. S13). Applying less L-Glu restricted the extent of systemic $[Ca^{2+}]_{cyt}$ increase; e.g., applying 50 mM L-Glu mimicked Ca^{2+} increases observed with wounding (compare fig. S12, B and C, and table S1).

To determine whether apoplastic Glu concentration ($[Glu]_{apo}$) was increased by wounding, we targeted the GFP-based Glu sensor iGluSnFR (*18*) to the cell wall (fig. S14 and movie S11). Upon wounding, the iGluSnFR signal increased locally at the cut region (Fig. 4, D and E, and movie S12), mirroring $[Ca^{2+}]_{cyt}$ dynamics at this site (fig. S15A). In vivo calibrations (fig. S14, C to E) suggested that $[Glu]_{apo}$ reached ~50 mM at the damaged site, consistent with reports that resting $[Glu]_{apo}$ is ~1 mM (*19*) and that releasable symplastic [Glu] in, e.g., the phloem is ~10 to 50 mM (*20, 21*). With greater leaf damage (hemostat crushing), Glu release to the apoplast was more extensive (fig. S15B and movie S13) and more distal leaves showed changes in $[Ca^{2+}]_{cyt}$ (table S1). Thus, the plant could tailor the extent of its systemic defense response to the severity of damage, possibly by adjusting $[Glu]_{apo}$ produced at the wound site(s).

Peptides, oligogalacturonides (OGs), adenosine 5′-triphosphate (ATP), and high mobility group (HMG) box domain–containing proteins have all been proposed as plant damage–associated molecular patterns (DAMPs), i.e., molecular elicitors of defense released upon wounding (*22*). We show here that Glu is also a DAMP, either leaking from damaged cells or actively released upon wounding. This Glu activates GLR ion channels, eliciting defense signal propagation through altered $[Ca^{2+}]_{cyt}$, with the vasculature as one key highway for transmission between organs. Despite links between the action of DAMPS to defense and Ca^{2+} signaling (*22*), application of neither OG nor the pathogen defense elicitor flg22 initiated systemic $[Ca^{2+}]_{cyt}$ increases (fig. S16), suggesting that Glu may be a critical signal in long-distance propagation of wound signaling events.

disrupted (Fig. 2D), reinforcing the likely role of PD in the spread of the $[Ca^{2+}]_{cyt}$ increase and triggering of the systemic response through target leaves.

Rapid propagation of systemic electrical signals depends upon GLR ion channel family members *GLR3.3* and *GLR3.6* (*3–5*); *glr3.3* and *glr3.6* single mutants showed altered kinetics of the propagating $[Ca^{2+}]_{cyt}$ signal, with *glr3.6* exhibiting the most severe reduction (fig. S10). Propagation was completely inhibited in the *glr3.3 glr3.6* double mutant (Fig. 3 and movie S7), but this response

was restored to nearly wild-type levels by driving *GLR3.6* expression in this line (Fig. 3, B and C, and movie S8), confirming the link between GLR function and propagation of the $[Ca^{2+}]_{cyt}$ increase.

GLR3.3 is ubiquitously expressed in roots, including the vasculature (*15*), and expressing *pGLR3.3::GLR3.3-EGFP* (enhanced green fluorescent protein) in the *glr3.3* background [*pGLR3.3:: GLR3.3-EGFP* functionally rescues *glr3.3* knockout phenotypes (*15*)] showed that GLR3.3 is localized to the phloem in leaves (Fig. 3D and fig. S11), consistent with a role of sieve tube Ca^{2+} channels

REFERENCES AND NOTES

1. G. A. Howe, I. T. Major, A. J. Koo, *Annu. Rev. Plant Biol.* **69**, 387–415 (2018).
2. W. G. Choi *et al.*, *Plant J.* **90**, 698–707 (2017).
3. S. A. Mousavi, A. Chauvin, F. Pascaud, S. Kellenberger, E. E. Farmer, *Nature* **500**, 422–426 (2013).

4. V. Salvador-Recatalà, W. F. Tjallingii, E. E. Farmer, *New Phytol.* **203**, 674–684 (2014).
5. V. Salvador-Recatalà, *Plant Signal. Behav.* **11**, e1161879 (2016).
6. B. G. Forde, M. R. Roberts, *F1000Prime Rep.* **6**, 37 (2014).
7. L. Tian *et al.*, *Nat. Methods* **6**, 875–881 (2009).
8. A. J. Koo, X. Gao, A. Daniel Jones, G. A. Howe, *Plant J.* **59**, 974–986 (2009).
9. G. Glauser *et al.*, *J. Biol. Chem.* **284**, 34506–34513 (2009).
10. W. J. Lucas *et al.*, *J. Integr. Plant Biol.* **55**, 294–388 (2013).
11. R. Hedrich, V. Salvador-Recatalà, I. Dreyer, *Trends Plant Sci.* **21**, 376–387 (2016).
12. J. Tilsner, W. Nicolas, A. Rosado, E. M. Bayer, *Annu. Rev. Plant Biol.* **67**, 337–364 (2016).
13. J. Y. Lee *et al.*, *Plant Cell* **23**, 3353–3373 (2011).
14. A. Levy, M. Erlanger, M. Rosenthal, B. L. Epel, *Plant J.* **49**, 669–682 (2007).
15. E. D. Vincill, A. E. Clarin, J. N. Molenda, E. P. Spalding, *Plant Cell* **25**, 1304–1313 (2013).
16. A. C. Furch *et al.*, *Plant Cell* **21**, 2118–2132 (2009).
17. E. E. Farmer, D. Gasperini, I. F. Acosta, *New Phytol.* **204**, 282–288 (2014).
18. J. S. Marvin *et al.*, *Nat. Methods* **10**, 162–170 (2013).
19. G. Lohaus, H. W. Heldt, *J. Exp. Bot.* **48**, 1779–1786 (1997).
20. E. Hunt *et al.*, *J. Exp. Bot.* **61**, 55–64 (2010).
21. J. Sandström, J. Pettersson, *J. Insect Physiol.* **40**, 947–955 (1994).
22. H. W. Choi, D. F. Klessig, *BMC Plant Biol.* **16**, 232 (2016).

Science

Glutamate triggers long-distance, calcium-based plant defense signaling

Masatsugu Toyota, Dirk Spencer, Satoe Sawai-Toyota, Wang Jiaqi, Tong Zhang, Abraham J. Koo, Gregg A. Howe and Simon Gilroy

Rapid, long-distance signaling in plants

A plant injured on one leaf by a nibbling insect can alert its other leaves to begin anticipatory defense responses. Working in the model plant *Arabidopsis*, Toyota *et al.* show that this systemic signal begins with the release of glutamate, which is perceived by glutamate receptor–like ion channels (see the Perspective by Muday and Brown-Harding). The ion channels then set off a cascade of changes in calcium ion concentration that propagate through the phloem vasculature and through intercellular channels called plasmodesmata. This glutamate-based long-distance signaling is rapid: Within minutes, an undamaged leaf can respond to the fate of a distant leaf.

Science, this issue p. 1112; see also p. 1068

ARTICLE TOOLS	http://science.sciencemag.org/content/361/6407/1112
SUPPLEMENTARY MATERIALS	http://science.sciencemag.org/content/suppl/2018/09/12/361.6407.1112.DC1
RELATED CONTENT	http://science.sciencemag.org/content/sci/361/6407/1068.full
REFERENCES	This article cites 35 articles, 11 of which you can access for free http://science.sciencemag.org/content/361/6407/1112#BIBL
PERMISSIONS	http://www.sciencemag.org/help/reprints-and-permissions

Use of this article is subject to the Terms of Service